DTU Library

Electromagnetic power flow between opposite sides of a lossy dielectric sphere using spherical vector wave expansion

Nour, Baqer; Breinbjerg, Olav

[Link back to DTU Orbit](#)

Electromagnetic power flow between opposite sides of a lossy dielectric sphere using spherical vector wave expansion

Baqer Nour[*], Olav Breinbjerg[+]

Department of Electrical Engineering, Electromagnetic Systems, Technical University of Denmark
Ørsteds Plads, building 348, DK-2800 Kgs. Lyngby, Denmark
[*]bn@elektro.dtu.dk, [+]ob@elektro.dtu.dk.

Abstract— **This article addresses the problem of communication in near field region. The proposed example is the communication between two small antennas, which are modelled as an electric dipole antenna (transmitter) and a small box (receiver), near a sphere that models a head. Spherical vector wave expansion SVWE is used to calculate the response of the model and to investigate propagation of power. Influence of the orientation of the antennas on the propagation is studied. The effect of location of the receiving antenna on the amount of the received power is investigated too.**

I. INTRODUCTION

Applications of wireless technology have found place in many areas. Recently they have been used in wireless sensors placed on a person, either for monitoring health information, [1] and [2], or for communication between hearing aids devices. Such devices are small in size and the power supply is limited. The impact of the environment is important in designing the antenna and deciding the working frequency. Communication channel of such an environment is not fully characterized, and the mechanisms of coupling are not clear. The example of hearing aids is taken, where two small antennas communicate to each other in presence of the head. The antennas are taken to be operating at wave lengths comparable to or larger than the diameter of the head.

A simple model is used to investigate the coupling. The head is modelled as a sphere, which represents the brain. The necessarily parameters are the conductivity and the permittivity of the brain, [3]. The transmitting antenna is modelled as electric dipoles.

The traditional free-space / plane wave propagation link-model is inapplicable for the configuration of two antennas on opposite sides of a head. Indeed, for this unusual radio communication link it is necessary to determine the coupling mechanisms; i.e. how power flows from one antenna to the other. For a hertzian z-polarized the electric dipole has components depend on $1/kr$, $1/(kr)^2$ and $1/(kr)^3$. Usually we ignore $1/(kr)^2$ and $1/(kr)^3$ at certain distance form the antenna. But these parts become significant at small distance, which is the case for hearing aids communications.

The sphere model is used to compute the electric and magnetic fields, at the same time it is used to compute the power intensity induced by electric dipole near the head. The fields are calculated using spherical wave expansions.

The article is organized to section II, which describes the geometry of the problem and the selected solution. Coefficients of the incident, scattered and total fields are mentioned. The powers dissipate in the dielectric sphere and the radiation power are given in term of the coefficients of the fields. Section III includes numerical results of the powers as a function of frequencies, and 2D plots of the power density for different frequencies and different orientations of the transmitting antenna. Transmission efficiency concept will be defined for communication between a transmitting antenna and receiving model of an antenna. Conclusions are given in section IV.

II. ANALYTICAL FORMULATION

The model consists of a hertzian dipole of *p*-polarization located on the z-axis at distance r' and a sphere that has the same parameters as the brain tissue and has radius r_{sph}, see Figure 1. The properties of the brain are taken from [3]. Two polarizations are considered, *x* and *z*. The sphere is centred at the origin of the coordinate system. The dipoles are shown as vectors. A receiving antenna, to collect the power on the other side of the sphere, is modelled as box located at same distance as the dipole at angle θ_{rec} with the z-axis. It is orthogonal to the sphere for the *z*-oriented dipole, and it is tangential for the *x*-oriented dipole.
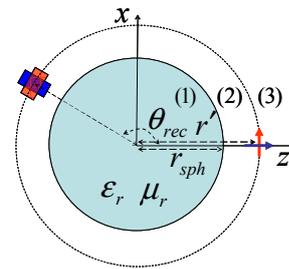
Fig. 1 The configuration of the model, which consists of a hertzian dipole of *p*-polarization (the red and blue arrows), and a sphere that has permittivity ε_r and conductivity σ_r. The sphere has radius r_{sph} and the dipole is located at distance r'. A receiver antenna (the red and the blue boxes) is located at distance r' and angle θ_{rec}.

The space is divided into three regions. Region 1 ($r < r_{sph}$) is the sphere, region 2 ($r_{sph} < r < r'$) is the free-space between

the sphere and the dipole and region 3 ($r > r'$) is the free-space outside the dipole. The incident field E^i of the dipole induces a scattering field E^s outside the sphere and a total field E^t inside the sphere.

The field intensities in each region are written as spherical vector wave expansions SVWE, [4], [5], [6] and [7]. The idea is to find coefficients that weight the spherical modes in the expansion. The coefficients are calculated for each mode using the boundary conditions at the interface of the regions. Electric and magnetic fields in a source-free region are given as, [5, A1.1 and A1.2]:

$$\vec{E}(r,\theta,\phi) = \frac{k}{\sqrt{\eta}} \sum_{csmn} Q_{smn}^{(c)} \vec{F}_{smn}^{(c)}(r,\theta,\phi) \tag{1a}$$

$$\vec{H}(r,\theta,\phi) = -ik\sqrt{\eta} \sum_{csmn} Q_{smn}^{(c)} \vec{F}_{3-s,mn}^{(c)}(r,\theta,\phi) \tag{1b}$$

$$\eta = \sqrt{\frac{\varepsilon}{\mu}} \qquad k = \omega\sqrt{\mu\varepsilon}$$

Time factor $\exp(-i\omega t)$ is used through this article. The spherical vector wave functions $\overline{F}_{smn}^{(c)}$ are defined in [5, A1.45 and A1.46].

A. Excitation and incident field

An electric hertzian dipole source is used to excite the model. Electric moment d_e of the dipole is taken to be constant. Two basic orientations of the dipole are used, x-oriented dipole (tangential to the sphere) and z-oriented dipole (orthogonal to the sphere). Any orientation can be realized by vector addition. The current density of the dipoles is $J = p \cdot d_e \cdot \delta(x)\,\delta(y)\delta(z-z')$, where p can be along x-direction or z-direction, $z' = r'$ and δ is the Dirac delta function.

The coefficients for the incident field are calculated using the reciprocity theorem, [5, A1.77 – A1.81]. The coefficients will be used to calculate the scattering field and the total field coefficients. SVWE model treats the space outside the dipole as two regions; inside and outside region. If we consider the problem of Figure 1 in absence of the sphere, the inside region is region 2 and the outside region is 3.

The coefficients of the x-oriented dipole are calculated to be:

$$Q_{11n}^{(c)i} = -id_e \frac{k_0}{\sqrt{\eta_0}} \frac{1}{4}\sqrt{\frac{2n+1}{\pi}} z_n^{(4-c)}(k_0 r') \tag{2}$$

$$Q_{1,-1,n}^{(c)i} = Q_{11n}^{(c)i} \tag{3}$$

$$Q_{21n}^{(c)i} = d_e \frac{k_0}{\sqrt{\eta_0}} \frac{1}{4}\sqrt{\frac{2n+1}{\pi}} \frac{1}{k_0 r'} \frac{d}{d(k_0 r')}\left\{ k_0 r' z_n^{(4-c)}(k_0 r') \right\} \tag{4}$$

$$Q_{2,-1,n}^{(c)i} = -Q_{21n}^{(c)i} \tag{5}$$

where $c = 1$ for $r < r'$ and $c = 3$ for $r > r'$ and k_0 and η_0 are the wave number and the intrinsic admittance of the free-space respectively. The function $z_n^{(c)}$ is the spherical Bessel function ($c = 1$), spherical Neumann function ($c = 2$), spherical Hankel function of the first kind ($c = 3$) or spherical Hankel function of the second kind ($c = 4$). The remaining coefficients are zero.

By same method the coefficients of the z-oriented dipole are calculated, all the coefficients are zero except for the following coefficients:

$$Q_{20n}^{(c)i} = -d_e \frac{k_0}{\sqrt{\eta_0}} \sqrt{\frac{n(n+1)(2n+1)}{4\pi}} \frac{z_n^{(4-c)}(k_0 r')}{k_0 r'} \tag{6}$$

B. Scattering by dielectric sphere

The incident field will be spherical Bessel functions ($c = 1$). The tangential components of the electric and the magnetic fields are continuous at the sphere surface:

$$\hat{r}\times\left(\vec{E}^i + \vec{E}^s\right) = \hat{r}\times\vec{E}^t$$
$$\hat{r}\times\left(\vec{H}^i + \vec{H}^s\right) = \hat{r}\times\vec{H}^t \tag{7}$$

The coefficients of the scattered and the total fields are calculated using the orthogonality property of SVWE [5, A1.69]. For an x-polarized dipole, the coefficients are:

$$Q_{11n}^s = Q_{11n}^{(1)i}$$
$$\cdot \frac{\sqrt{\frac{\eta_0}{\eta_1}} R_{1n}^{(1)}(k_0 r_{sph}) R_{2n}^{(1)}(k_0 r_{sph}) - \sqrt{\frac{\eta_1}{\eta_0}} R_{2n}^{(1)}(k_1 r_{sph}) R_{1n}^{(1)}(k_0 r_{sph})}{\sqrt{\frac{\eta_1}{\eta_0}} R_{2n}^{(1)}(k_1 r_{sph}) R_{1n}^{(3)}(k_0 r_{sph}) - \sqrt{\frac{\eta_0}{\eta_1}} R_{1n}^{(1)}(k_1 r_{sph}) R_{2n}^{(3)}(k_0 r_{sph})} \tag{8}$$

$$Q_{21n}^s = Q_{21n}^{(1)i}$$
$$\cdot \frac{\sqrt{\frac{\eta_0}{\eta_1}} R_{2n}^{(1)}(k_1 r_{sph}) R_{1n}^{(1)}(k_0 r_{sph}) - \sqrt{\frac{\eta_1}{\eta_0}} R_{1n}^{(1)}(k_1 r_{sph}) R_{2n}^{(1)}(k_0 r_{sph})}{\sqrt{\frac{\eta_0}{\eta_1}} R_{1n}^{(1)}(k_1 r_{sph}) R_{2n}^{(3)}(k_0 r_{sph}) - \sqrt{\frac{\eta_1}{\eta_0}} R_{2n}^{(1)}(k_1 r_{sph}) R_{1n}^{(3)}(k_0 r_{sph})} \tag{9}$$

$$Q_{11n}^t = Q_{11n}^{(1)i} \frac{k_0}{k_1}$$
$$\cdot \frac{R_{1n}^{(1)}(k_0 r_{sph}) R_{2n}^{(3)}(k_0 r_{sph}) - R_{2n}^{(1)}(k_0 r_{sph}) R_{1n}^{(3)}(k_0 r_{sph})}{\sqrt{\frac{\eta_0}{\eta_1}} R_{1n}^{(1)}(k_1 r_{sph}) R_{2n}^{(3)}(k_0 r_{sph}) - \sqrt{\frac{\eta_1}{\eta_0}} R_{2n}^{(1)}(k_1 r_{sph}) R_{1n}^{(3)}(k_0 r_{sph})} \tag{10}$$

$$Q_{21n}^t = Q_{21n}^{(1)i} \frac{k_0}{k_1}$$
$$\cdot \frac{R_{2n}^{(1)}(k_0 r_{sph}) R_{1n}^{(3)}(k_0 r_{sph}) - R_{1n}^{(1)}(k_0 r_{sph}) R_{2n}^{(3)}(k_0 r_{sph})}{\sqrt{\frac{\eta_0}{\eta_1}} R_{2n}^{(1)}(k_1 r_{sph}) R_{1n}^{(3)}(k_0 r_{sph}) - \sqrt{\frac{\eta_1}{\eta_0}} R_{1n}^{(1)}(k_1 r_{sph}) R_{2n}^{(3)}(k_0 r_{sph})} \tag{11}$$

$$Q_{1,-1,n}^s = Q_{11n}^s, \quad Q_{2,-1,n}^s = -Q_{21n}^s$$
$$Q_{1,-1,n}^t = Q_{11n}^t, \quad Q_{2,-1,n}^t = -Q_{21n}^t \tag{12}$$

$$R_{sn}^{(c)}(kr) = \begin{cases} z_n^{(c)}(kr) & s = 1 \\ \dfrac{1}{kr}\dfrac{d}{d(kr)}\left\{kr z_n^{(c)}(kr)\right\} & s = 2 \end{cases} \tag{13}$$

k_1 and η_1 are the wave-number and the intrinsic admittance of the sphere ($r < r_{sph}$) respectively. For a z-polarized dipole the coefficients become:

$$Q_{20n}^s = Q_{20n}^{(1)i}$$

$$\cdot \frac{\sqrt{\frac{\eta_1}{\eta_0}} R_{2n}^{(1)}(k_0 r_{sph}) R_{1n}^{(1)}(k_1 r_{sph}) - \sqrt{\frac{\eta_0}{\eta_1}} R_{1n}^{(1)}(k_0 r_{sph}) R_{2n}^{(1)}(k_1 r_{sph})}{\sqrt{\frac{\eta_0}{\eta_1}} R_{1n}^{(3)}(k_0 r_{sph}) R_{2n}^{(1)}(k_1 r_{sph}) - \sqrt{\frac{\eta_1}{\eta_0}} R_{2n}^{(3)}(k_3 r_{sph}) R_{1n}^{(1)}(k_1 r_{sph})}$$

$$(14)$$

$$Q_{20n}^t = Q_{20n}^{(1)i} \frac{k_0}{k_1}$$

$$\cdot \frac{R_{1n}^{(3)}(k_0 r_{sph}) R_{2n}^{(1)}(k_0 r_{sph}) - R_{2n}^{(3)}(k_0 r_{sph}) R_{1n}^{(1)}(k_0 r_{sph})}{\sqrt{\frac{\eta_0}{\eta_1}} R_{1n}^{(3)}(k_0 r_{sph}) R_{2n}^{(1)}(k_1 r_{sph}) - \sqrt{\frac{\eta_1}{\eta_0}} R_{2n}^{(3)}(k_3 r_{sph}) R_{1n}^{(1)}(k_1 r_{sph})}$$

$$(15)$$

C. Power calculations

The power delivered by the dipole P_{del} is the sum of the power dissipated in the sphere P_{dis} and the far-field radiated power P_{rad}. It is noted that the delivered power P_{del} varies with the parameters of the sphere and it is different from the well-known power by a dipole in free space ($\omega \mu_0 k_0 d_e^2 / 12\pi$). The dissipated power and the radiated power will be calculated using the poynting vector:

$$P_{dis} = -\text{Re}\left\{ \frac{1}{2} \oint_{S_1} \vec{E}^t \times \vec{H}^{t*} \cdot d\vec{S} \right\} \tag{16}$$

$$P_{rad} = \text{Re}\left\{ \frac{1}{2} \oint_{S_2} (\vec{E}^i + \vec{E}^s) \times (\vec{H}^i + \vec{H}^s)^* \cdot d\vec{S} \right\} \tag{17}$$

$$P_{del}^x = P_{dis}^x + P_{rad}^x \tag{18}$$

Here S_1 is the surface of the sphere and S_2 is a far-field sphere. The powers for the x-oriented dipole are:

$$P_{dis}^x = -\text{Re}\left\{ ir^2 |k_1|^2 \frac{(\sqrt{\eta_1})^*}{\sqrt{\eta_1}} \sum_{n=1}^N \left[|Q_{11n}^t|^2 R_{1n}^{(1)} R_{2n}^{(1)*} \right. \right.$$
$$\left. \left. - |Q_{21n}^t|^2 R_{2n}^{(1)} R_{1n}^{(1)*} \right] \right\} \tag{19}$$

$$P_{rad}^x = 2\text{Re}\left\{ \sum_{n=1}^N \left[|Q_{11n}^{(3)i} + Q_{11n}^s|^2 + |Q_{21n}^{(3)i} + Q_{21n}^s|^2 \right] \right\} \tag{20}$$

$$R_{sn}^{(1)} = R_{sn}^{(1)}(k_1 r_{sph}) \tag{}$$

The powers for the z-oriented dipole are:

$$P_{dis}^z = \text{Re}\left\{ i\frac{1}{2} r^2 |k_1|^2 \frac{(\sqrt{\eta_1})^*}{\sqrt{\eta_1}} \sum_{n=1}^N \left[R_{1n}^{(1)} R_{2n}^{(1)*} |Q_{20n}^t|^2 \right] \right\} \tag{21}$$

$$P_{rad}^z = \text{Re}\left\{ \sum_{n=1}^N |Q_{20n}^{(3)i} + Q_{20n}^s|^2 \right\} \tag{22}$$

III. Results and Discussion

The power flow is investigated in different ways: 1) inspection of the 2D plot of the magnitude and direction of the power flow density and 2) the power entering the surfaces of the receiving antenna.

Figure 2 shows, at frequencies 400 MHz and 4 GHz, the normalized wave impedances of the total field (sum of the incident and the scattered fields outside the sphere) and normalized wave impedances of the incident field. The normalized wave impedance is the ratio of the magnitude of electric and magnetic fields, normalized to the intrinsic impedance of the medium.
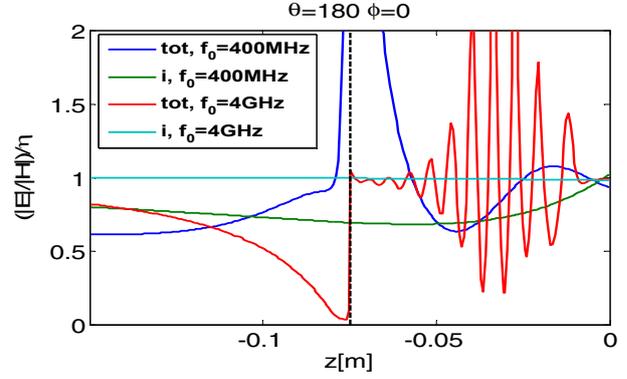

Fig. 2 Normalized wave impedances of the total fields at frequencies 400 MHz (blue line) and 4 GHz (red line), and the incident fields at 400 MHz (green line) and 4GHz (cyan line). η is the intrinsic impedance of the free-space for the incident fields, while for the total field it is the intrinsic impedance of the sphere and the free-space for observation points inside and outside the sphere respectively. The dashed line is the surface of the sphere.

At 400 MHz the normalized wave impedance of the total field varies around one inside the sphere ($z > -0.075$m), and it is high at the surface of the sphere and less than 1 outside the surface. Both inside and outside the sphere, the normalized wave impedance of the total field oscillates around the normalized wave impedance of incident field. At 4 GHz the normalized impedance of total field oscillates more rapidly with distance, and it converges to 1 near the inside surface and it less than 1 outside the surface.

For plane wave propagation the normalized wave impedance equals 1. Thus Figure 2 clearly shows that the field inside and outside the sphere is far more complicated than a plane wave. This is the case for the incident field of 400 MHz because we are in the near-field of the dipole, while the incident field for 4 GHz shows plane wave property. For both frequencies the total field, inside and outside the sphere, deviates significantly from a plane wave.

The radiated and dissipated powers are frequency dependent. In Figure 3 the radiated and dissipated power are calculated for different frequencies and different orientations of the dipole. The vertical axis shows the radiated and dissipated power normalized to the delivered power of the dipole, which can be oriented in x or z directions, and the horizontal axis is the operation frequency in MHz. The dissipation is larger at the low frequencies, while at high frequencies the radiation becomes dominant. The normalized radiated power is higher for the z-oriented dipole than the x-oriented dipole. While for the z-oriented dipole the

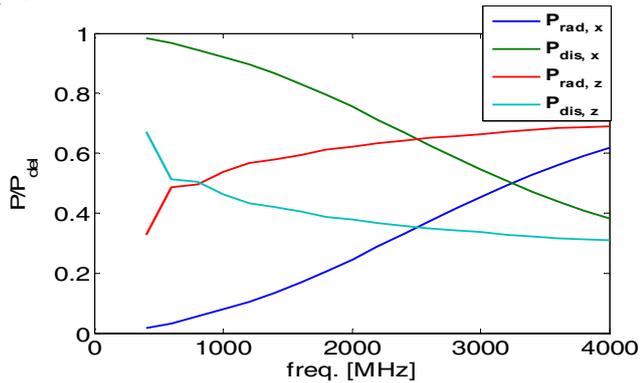normalized dissipated power is smaller than the x-oriented dipole.

Fig. 3 Dissipated power P_{dis} and radiated power P_{rad} normalized to delivered power P_{del} vs. frequency for x- and z-oriented dipoles.

The decrease of the dissipated power can be explained in two ways; 1) as the frequency increases the ratio of the conductivity to the frequency decrease, so the attenuation becomes smaller. The loss tangent of the sphere at 400 MHz and 4 GHz are $Im\{\varepsilon\}/Re\{\varepsilon\} = 0.755$ and 0.285 respectively, and 2) a small amount of the delivered power penetrates the sphere while most of the power reflects back from the sphere. The reflection coefficients at 400 MHz and 4 GHz are 0.79 and 0.86 respectively.

The presence of the sphere near the dipole redistributes the power flow density. Figures 4 and 5 show the power flow density at 400 MHz for x- and z-polarized dipoles respectively, where the power density is normalized to the delivered power.
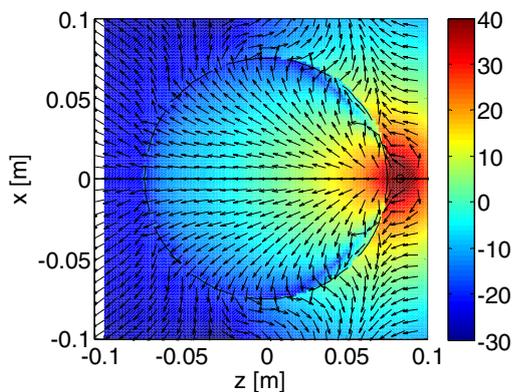

Fig. 4 Normalized power density for the sphere and an x-oriented hertzian dipole works at 400 MHz. The colour is the magnitude (dB/m^2) and the directions are indicated by arrows. The location of the hertzian dipole is shown as a small black circle in the right side.

The colours are the magnitude (dB/m^2) of the normalized power flow density and the direction of the power flow density is indicated by arrows. In both orientations the power flows inside and outside the sphere. A large magnitude of power density is concentrated in a small area near the antenna. This area will be called hot spot, which is characterized by a dark red colour.

The x-oriented dipole has a large hot spot. The inside power propagates through the sphere in almost radial lines from the area close to the dipole. The power decreases very rapidly as it propagates through the sphere. There is a jump in power density between the inside and the outside regions near the surface of the sphere since the tangential component is not necessarily continuous. At left side of the sphere the power flows out of the sphere.

The z-oriented dipole has a small hot spot. The inside power flow density propagates toward the poles region. The magnitude of the inside power flow density declines as it propagates and it is null along the z-axis, which is expected for the z-oriented dipole. The magnitude of the power density jumps at the surface of the sphere. The outside power flows along the surface of the sphere to the poles, and then it flows in the negative z-direction. The magnitude of the power flow density, that bounds the sphere, is larger than the case of the x-oriented dipole.
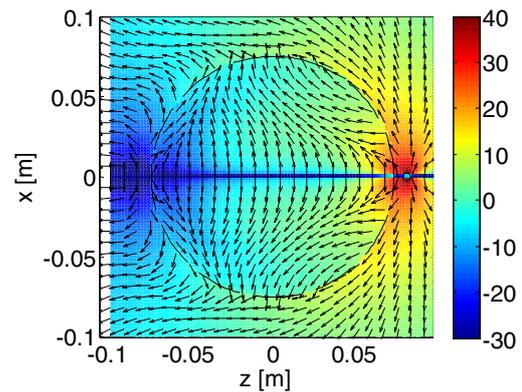

Fig. 5 Normalized power density for a z-oriented hertzian dipole works at 400 MHz.

Since the dipole is close to the sphere, the surface of the sphere acts as a ground plane to the dipole. So the image theory can be applied here. The image of the x-oriented dipole has destructive effect on the radiated power. Most of the power is concentrated inside the region between the dipole and its image, at same time the decreasing of the power becomes faster with the distance. While the image of the z-oriented dipoles has a constructive effect on the radiation of the dipole, so there is small hot spot around the dipole.

The jump in power density, at the surface of the sphere, supports the idea that power flows inside and along the surface. Since the normal power flow has to be continues through the surface of the sphere, the extra power at the outside surface is the power that flows along the surface of the sphere; the directions of arrows shows this phenomenon in all figures of the normalized power density.

Figure 6 and 7 shows the normalized power density of an x- and z-oriented dipoles operate at 4 GHz. The inside power flow density is focused in narrow beam and less amount of power flow density propagates inside the sphere than the case of 400 MHz. At same time magnitude of the power density bounding the sphere becomes larger, and the sphere reflects back more power toward the antenna as the arrows show.
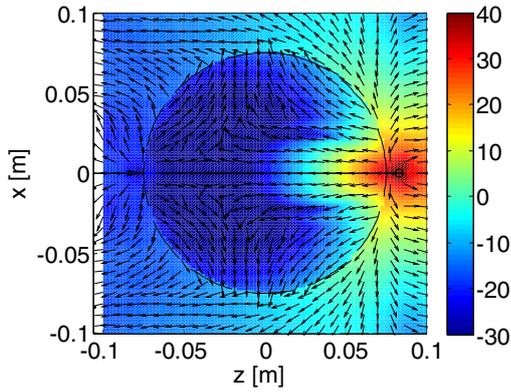
Fig. 6 The normalized power density for an *x*-oriented hertzian dipole works at 4 GHz.
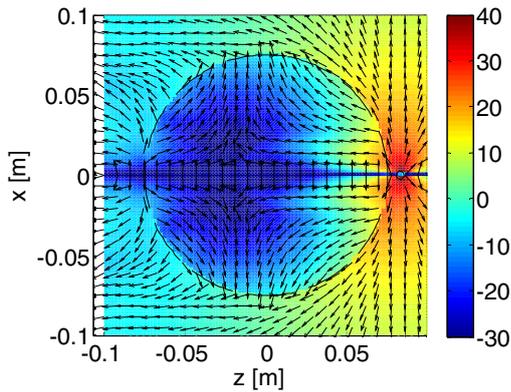

Fig. 7 The normalized power density for a *z*-oriented hertzian dipole works at 4 GHz.

The receiver antenna model is a rectangular box and has the following dimensions 1.5 cm x 0.5 cm x 0.5 cm. The antenna receives a power P_{rec}, which is calculated by integrating the power density that enters the surfaces over the surfaces of the box. The ratio of the received power to the delivered power will be called the transmission efficiency. Figure 8 shows the transmission efficiency, as a function of the location angle θ_{rec}, for the *x*- and *z*-oriented dipoles.
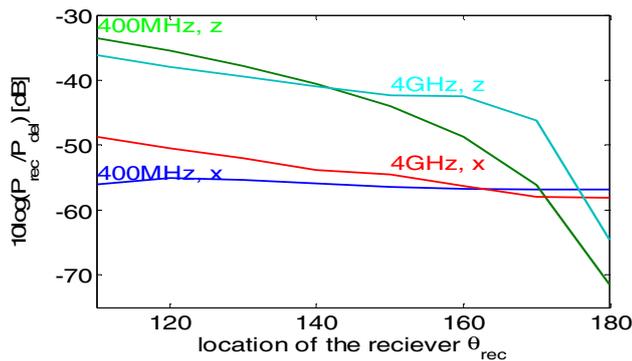

Fig. 8 The power received by a box, with dimensions 1.5cm x0.5cm x 0.5 cm, at frequencies 400 MHz and 4 GHz as a function of the location angle θ_{rec}. The distance form the sphere model to the center of the sphere and the box is 0.75 cm. Letters *x* and *z* stand for *x*- and *z*-orientation of the dipole.

The transmission efficiency of the *z*-oriented dipole is more sensitive to the location angle θ_{rec} than the *x*-oriented dipole. The *z*-oriented dipole has higher transmission efficiencies in general than the *x*-oriented dipole. This effect can also be seen from the power flow density Figures 4 to 7.

IV. CONCLUSIONS

The power flow is investigated near a lossy dielectric sphere. The analysis is based on the spherical vector wave expansion. Two orientations are studied, *x*-and *z*-oriented hertzian dipoles. The normalized wave impedances show the complex nature of the propagation near the sphere. The propagation is far from being a plane wave.

The dissipated and radiated powers are frequency related. The dissipation is large at low frequencies and becomes smaller at high frequencies. While the radiated power increases with increasing the frequency. The z-oriented dipole causes less dissipation in the sphere and higher radiation than the *x*-oriented dipole.

The sphere acts as ground for the dipole. So hot spot region is located between the dipole and the sphere. The size of the hot spot area depends on the orientation and the frequency of the dipole.

The transmission efficiency, between the dipole and the receiving box, is investigated vs. location angle, orientation and frequency. The z-oriented dipole gives higher transmission efficiency values in general, except for location angles close to 180 degree. The transmission efficiency becomes high as the receiving model displaces from the *z*-axis.

REFERENCES

[1] T. Zasowski, G. Mayer, F. Althaus, A. Wittneben, "UWB Signal Propagation at the Human Head," *IEEE Trans on Microwave Theory and Techniqes* ., vol. 54, No. 4, pp. 1836–1844, April 2006.

[2] A. Fort, C. Desset, J. Rychaert, P. D. Doncker, L. V. Biesen, S. Donnay, "Ultra Wide-band Area Channel Model," IEEE International Conference on Communicatios *ICC 2005*, Seoul, 16-20 May 2005, pp. 2840-2844.

[3] P. J. Dimbylow, O. P. Gandhi, "Finite-difference time-domain calculations of SAR in a realistic heterogeneous model of the head for plane-wave exposure from 600 MHz to 3," *Phys. Med. Biol..*, vol. 36, No. 8, pp. 1075–1089.

[4] Arthur L. Aden, Milton Kerker, "Scattering of Electromagnetic Waves from Two Concentric Spheres," *Journal of Applied Phyics.*, vol. 22, No. 10, pp. 1242-1246, Oct. 1951.

[5] J. E. Hansen, *Spherical Near-Field Antenna Measurements*, Peter Peregrinus Ltd. London, United Kingdom: Short Run Press Ltd., 1988.

[6] J. A. Stratton, *Electomagnetic Theory*, Donald G Dudley, Series Editor, The IEEE Press Series on Electromagnetic Wave Theory.

[7] John H. Bruning, Yuen T. Lo, "Multiple Scattering of EM Waves by Spheres: Part I –Multipole Expansion and Ray-Optical Solutions," *IEEE Trans on Antennas and Propagation Propagation* ., vol. AP-19, No. 3, pp. 378–390, May 1971.